

Dynamics of electron excitation

Studies of the evolution of electronic states in the single-atom, two-electron systems are a first step toward understanding the transitions that occur in chemical reactions.

Ugo Fano

A key step in any chemical reaction is the transition of bonding electrons from one stable wave-mechanical state to another. A complete description of the evolution of states in the course of such transitions remains a distant goal—in spite of our rather extensive knowledge of chemical reactions. This article reviews a start on this problem that has been made in recent years.

Note at the outset that wave phenomena generally show remarkable stability under changes of the forces or boundary conditions that control them. Indeed, Niels Bohr remarked in the early days of quantum physics that the structural stability of matter rests on the separation of the energy levels of bonding electrons. Thus a single fact of physics accounts for a major feature of our world: stability. We could include, as an example of stability, the fact that each of us looks much the same for many years; yet we come from dust and return to dust, reminding us that the stability of molecular ground states is in fact circumvented in the course of molecular reactions.

A precondition for reactions is that the energy gap between two electronic levels must shrink to near degeneracy—for example, at certain nuclear configurations—but it remains to be seen how the electrons can then pass, for example, from a state identified by one set of quantum numbers to a state identified by a different set. Once activation energy is available and other constraints are removed, the evolution leading to a transition might conceivably proceed in such a complex manner as to defy description. Here we shall instead describe, as a relatively simple example, the excitation of a single

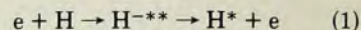
atom. In this case the evolution follows a smooth and predictable course, except for a critical point when the electronic system traverses a certain unstable configuration. The example is meant to serve as a prototype for later studies of electron transitions in chemical reactions.

The stability of stationary states was first studied in detail for the simplest system of all, the single-electron hydrogen atom, the stability of other systems being then accounted for in terms of independent-electron states. Transformations of states, on the other hand, depend inherently on the forces between electrons and on the resulting electron correlations. Hence the simplest prototypes for our study consist of two electrons, with sufficient energy to evolve from one stable state to another. Figure 1 shows a diagram of alternative transformations of such prototypes. It emphasizes that alternative reactions proceed through a common intermediate in which both electrons are excited. We will show how characteristics of an initially stable state tend to persist in the course of evolution through the intermediate stage but may change rather suddenly when the electrons pass through positions symmetrical with respect to the nucleus. This result may have broad significance; that is, it should hold for a wide class of processes because it stems from dimensional and topological considerations. We regard it as a general manifestation of the stability of wave patterns (which strikes us in the example of water surfaces, say), breaking only under the influence of localized disturbances.

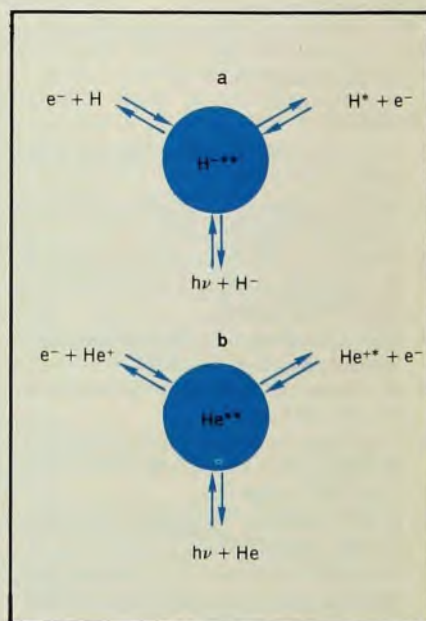
Initial evidence

The most familiar process, among those shown in figure 1, is the excitation of hydrogen by impact of a low-energy electron,

indicated by



The intermediate symbol, H^{**} , emphasizes that the electrons tend to remain correlated when most of the incident energy has been spent in dislodging the H electron from its ground state and the electrons move away from the nucleus with comparable velocities. (The most likely outcome is, however, the elastic collision indicated in the figure by $e + H \rightleftharpoons H^{**}$, in which the doubly excited intermediate may not manifest itself because the H electron need not be actually dislodged.)

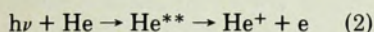


Alternative reactions in the two-electron systems H^- (figure 1a) and He (figure 1b). Note in each case the intermediate doubly excited complex. (Redrawn from *Atomic Physics* 4, 48, 1975.)

Figure 1

Ugo Fano is a professor of physics at the University of Chicago.

While understanding the process of excitation by collision is indeed our main goal, important evidence has resulted from observation of the helium process in figure 1b

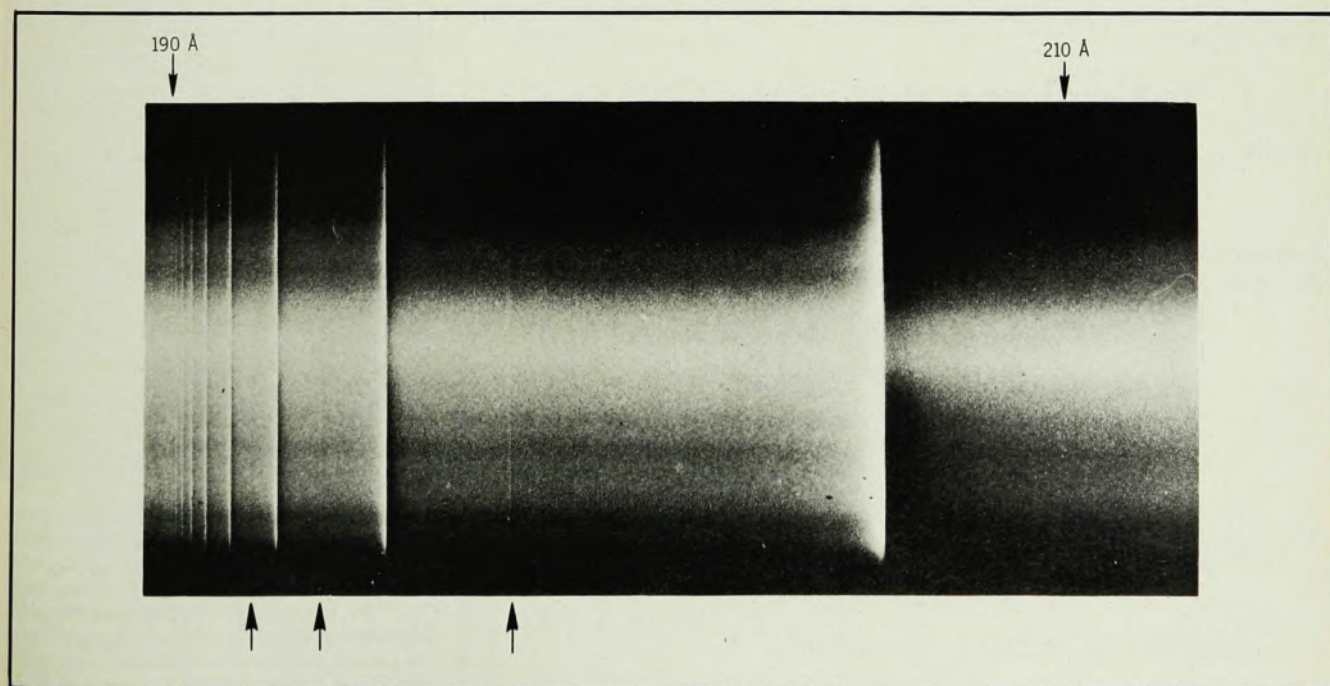


as a function of photon energy in the range 60–65 eV. Its cross section exhibits a Rydberg series of intense, sharp resonances converging to the 65.4 eV threshold for the final excited state He^{**} ($n = 2$) + e. (See the spectrogram in figure 2.) These resonances were attributed to temporary formation of discrete states of the doubly excited intermediate, He^{**} ,

which autoionize into He^+ ($n = 1$) + e after approximately 100 orbital periods.

The significance of these findings emerges from the following considerations. Photoabsorption by helium in its ground state leads to states with the spectroscopic designation $^1\text{P}^0$, that is, with $S = 0, L = 1$ and odd parity. These labels however, are insufficient to identify the excited state. In the usual independent-electron approximation of spectroscopy, the classification of final states would be completed by a configuration symbol consisting of the (n, l) quantum numbers of each electron. Three alternative series of configurations can yield

$^1\text{P}^0$ levels in the 60–65 eV range, namely (2s, np), (2p, ns) and (2p, nd), and the first two of these should be formed, according to this view, with comparable probabilities higher than the probability of the third one. The initial observation of only a *single* intense series represented a *qualitative* departure from this expectation and raised the question: How do the two excited electrons correlate instead of remaining approximately independent? Tentatively, the states responsible for the observed resonances were characterized as superpositions of configurations (2s, np) and (2p, ns) with equal weights and with phases that yield joint



The photoabsorption spectrum of helium between 190 and 210 Å. Note the two series of resonances, one intense, the other fainter and sharper.

Three faint lines are here marked with arrows. (From R. P. Madden and K. Codling, *Astrophys. J.* **141**, 364; 1965.)

Figure 2

in-step radial oscillations of the two electrons. Orthogonal superpositions should yield states with out-of-step oscillations, observable as fainter and sharper resonances additional to the intense series already seen. This prediction was soon verified (two or three of the fainter lines are just visible in the spectrogram reproduced in figure 2), but the task remained to develop the tentative

guess into a solid theory.

The details of this argumentation do not matter here; it was the bare essentials of the initial experiments and discussion that sparked the later work. The photoabsorption of helium in a new spectral range had afforded us a first glimpse of the behavior of a pair of electrons that remain correlated for appreciable time while free from the constraints that pre-

vail in a ground shell. The energy levels of this pair appeared to form regular series distinguished by widely different rates of formation and decay but by no recognized mechanical property. Extreme departures from the usual picture of quasi-independent electrons were apparent. To construct a new alternative picture we had to decipher the message contained in fragmentary information.

Because the Schrödinger equation for two electrons is accessible to numerical solution, the initial findings on He** stimulated extensive calculations by different authors and by different methods. (The successful work of Philip Burke encompassed also the resonances in the elastic collision processes $e + \text{He}^+ \rightleftharpoons \text{He}^{**}$, $e + \text{H} \rightleftharpoons \text{H}^{**}$ as well as the inelastic process leading to $e + \text{H}^*$.) The results agreed with the experimental observations and extended them greatly by establishing the following general pattern: For any given set of good quantum numbers (S , L and parity), *alternative* series of quasi-stationary states occur, whose probabilities of formation and decay are small and *differ* from series to series by one or two orders of magnitude. The calculations, however, gave no inkling of the mechanisms that generate series of such disparate properties, because they yielded all doubly excited states with

Analytical details

Equation 3 (Schrödinger equation for a two-electron atom):

$$\left\{ \frac{d^2}{dR^2} - \left[\frac{1}{R^2} \left(-\frac{d^2}{d\alpha^2} - \frac{1}{4} + \frac{l_1^2}{\cos^2 \alpha} + \frac{l_2^2}{\sin^2 \alpha} \right) - \frac{C(\alpha, \theta_{12})}{R} \right] + 2E \right\} (R^{5/2} \sin \alpha \cos \alpha \Psi) = 0$$

← U(R) →
↑ ↑ ↑
 MOCK CENTRIFUGAL • CENTRIFUGAL • COULOMB

Macek separation of variables

$$R^{5/2} \sin \alpha \cos \alpha \Psi = \sum_{\mu'} \phi_{\mu'}(R; \alpha, \hat{\mathbf{r}}_1, \hat{\mathbf{r}}_2) F_{\mu'}(R) \quad \text{General form}$$

$$\approx \phi_{\mu}(R; \alpha, \hat{\mathbf{r}}_1, \hat{\mathbf{r}}_2) F_{\mu}(R) \quad \text{Approximate form}$$

$$U(R) \phi_{\mu} = U_{\mu} \phi_{\mu}$$

Expression of Coulomb potential function of equation 3 for two electrons in the field of a nucleus of atomic number Z :

$$-C(\alpha, \theta_{12}) = R \left(-\frac{2Z}{r_1} - \frac{2Z}{r_2} + \frac{2}{|\mathbf{r}_2 - \mathbf{r}_1|} \right)$$

$$= -\frac{2Z}{\cos \alpha} - \frac{2Z}{\sin \alpha} + \frac{2}{(1 - \sin 2\alpha \cos \theta_{12})^{1/2}}$$

Transformation of equation 3 into a system of ordinary differential equations.

Introduce for each value of R a complete orthonormal set of functions $\Phi(R; \alpha, \hat{\mathbf{r}}_1, \hat{\mathbf{r}}_2)$:

$$\int_0^{\pi/2} d\alpha \int_{4\pi} d\hat{\mathbf{r}}_1 \int_{4\pi} d\hat{\mathbf{r}}_2 \Phi_{\mu'}^*(R; \alpha, \hat{\mathbf{r}}_1, \hat{\mathbf{r}}_2) \Phi_{\mu}(R; \alpha, \hat{\mathbf{r}}_1, \hat{\mathbf{r}}_2) = \delta_{\mu\mu'}$$

Expand:

$$R^{5/2} \sin \alpha \cos \alpha \Psi = \sum_{\mu'} \Phi_{\mu'}(R; \alpha, \hat{\mathbf{r}}_1, \hat{\mathbf{r}}_2) F_{\mu'}(R)$$

Substitution into equation 3, multiplying by Φ_{μ} and integrating over $\alpha, \hat{\mathbf{r}}_1$ and $\hat{\mathbf{r}}_2$, yields:

$$\left[\frac{d^2}{dR^2} + 2E \right] F_{\mu}(R) - \sum_{\mu'} [U_{\mu\mu'}(R) - W_{\mu\mu'}(R)] F_{\mu'}(R) = 0$$

with

$$U_{\mu\mu'}(R) = \langle \Phi_{\mu} | U(R) | \Phi_{\mu'} \rangle$$

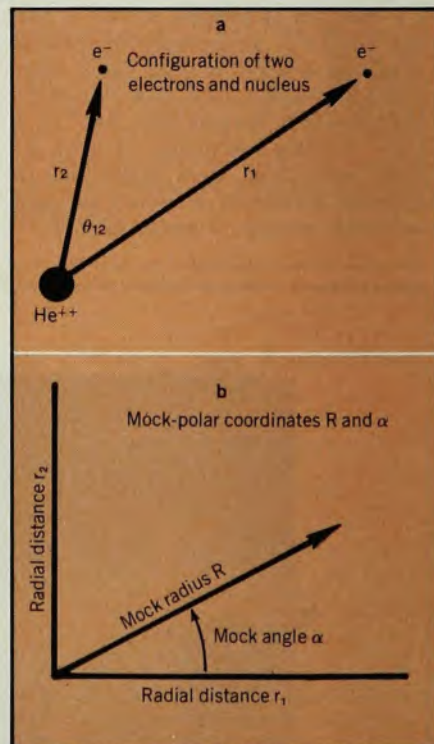
$$W_{\mu\mu'}(R) = 2 \left\langle \Phi \left| \frac{\partial \Phi_{\mu'}}{\partial R} \right\rangle \frac{d}{dR} + \left\langle \Phi_{\mu} \left| \frac{\partial^2 \Phi_{\mu'}}{\partial R^2} \right\rangle \right.$$

This equation reduces to equation 5 if:

► The functions Φ_{μ} are eigenfunctions of $U(R)$, whereby

$$U_{\mu\mu'}(R) = U_{\mu}(R) \delta_{\mu\mu'}$$

► The matrix elements $W_{\mu\mu'}(R)$ are disregarded.



Coordinate systems for the two-electron reactions of figure 1. Part a shows the conventional configuration with two electrons at r_1 and r_2 from the nucleus, with radius vectors making angle θ_{12} . Part b shows "mock polar" coordinates (R, α), in which angle θ_{12} does not appear; R acts as a scale parameter, while mock angle α ($\equiv \tan^{-1} r_2/r_1$) measures the "skewness" of diagram 3a. (Adapted from *Atomic Physics* 4, 50, 1975.)

Figure 3

Important news about PGT Intrinsic Germanium Coaxial Detectors

now you can have an IG coax with

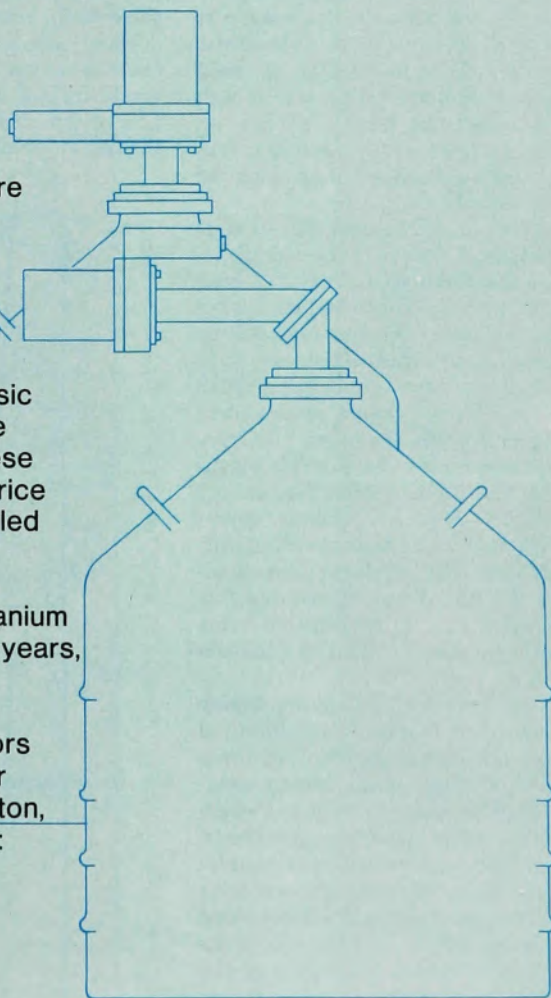
- Minimum Efficiency 5%
- Resolution
 - ≤ 1.90 keV (FWHM) } @ 1.33 MeV
 - ≤ 3.60 keV (FWTM) }
 - ≤ 0.80 keV (FWHM) @ 122 keV
- Unlimited Cycling to Room Temperature
- Stock Delivery
- **Full TWO year warranty**
- At a price of

\$7,850*

As pioneers in the development of Intrinsic Germanium Detectors, PGT's experience and success now permits us to offer these detectors at this dramatically reduced price and at the same time to offer an unequalled **two year warranty**.

If you already own a PGT Intrinsic Germanium Detector, purchased within the past two years, our **two year** warranty is retroactive.

For more information about PGT Detectors contact your local PGT representative or Princeton Gamma-Tech, Box 641, Princeton, N.J. 08540, Phone 609 924-7310. Cable: PRINGAMTEC. Telex: 843486.



 **P|G|T**
PRINCETON GAMMA-TECH

...for the best in detector technology

*U.S. Domestic Price

given (S, L , parity) in a single batch; the existence of series emerged only from analysis of the results, much as it does for experimental observations. In fact, the procedure at this stage could be described as "fruitful numerical experimentation." A full theory would provide instead an algorithm that yields each series separately and characterizes it by appropriate quantum numbers corresponding to new quasi-constants of the motion. The challenge raised by this situation has stimulated efforts extending over the last ten years and still in progress.

Quantum numbers and separability

As an introduction to the search for new quantum numbers, let us recall the meaning of the set of quantum numbers (n, l, m) that identifies stationary states of a spinless particle in a central field. The Schrödinger equation for this particle is fully separable in polar coordinates (r, θ, φ)—that is, it has eigenfunctions of the form $R_{nl}(r)\Theta_{lm}(\theta)\Phi_m(\varphi)$. Real eigenfunctions represent standing waves; in this case Φ_m has m nodes, Θ_{lm} has $l - m$ nodes and R_{nl} has $n - l - 1$. The larger the number of nodes of any of these functions, the shorter is its wavelength and the larger the kinetic energy—in other words, more nodes mean more excitation of the particle's motion along the pertinent coordinate.

Perturbations of the field that spoil its central symmetry change the eigenfunctions to a non-factorable form. For weak perturbations, which are in fact always present, the eigenfunctions may still be represented as superpositions of one term $R_{nl}\Theta_{lm}\Phi_m$ (or of a few terms) and of small corrections. This approach retains some significance for the quantum numbers, which still serve to characterize eigenfunctions and the corresponding energy eigenvalues. However, strong asymmetric perturbations wipe out the significance of quantum numbers; each eigenfunction is then fully identified, but this identification has no descriptive value comparable to that provided by quantum numbers.

What we have seen about the double excitations of He and of H^- implies then that the Schrödinger equation of these systems should be approximately separable, though we don't know yet in which coordinates. The small probabilities of formation and autoionization of double-excited states should result from whatever terms of the Hamiltonian are disregarded to make it separable. As in the case of the central field, a study of the nodes of the solutions of the separable equation should illustrate the mechanics of the doubly excited states.

Macek's construction

We consider now coordinates that prove useful for describing electron correlations. Figure 3a represents the joint position of two electrons and a nucleus,

that is, a "configuration" of a two-electron atom. A wavefunction of this atom depends in general on all variables of this diagram as well as on the diagram's orientation in space. The wave function's dependence on the angle θ_{12} represents the angular correlation of the electrons, while its dependence on the pair of radial distances (r_1, r_2) represents radial correlations, insofar as the wavefunction itself does not factor into separate functions of r_1 and r_2 . Figure 3b shows how the pair of radial variables (r_1, r_2) may be replaced by the equivalent pair (R, α). Of these, R represents the scale parameter of figure 3a, while α indicates the "skewness" of that triangular diagram, in that the triangle is isosceles for $\alpha = 45^\circ$ (i.e., for $r_1 = r_2$) and extremely skew for α near to 0° or 90° . In other words, angle $\alpha \equiv \tan^{-1} r_2/r_1$.

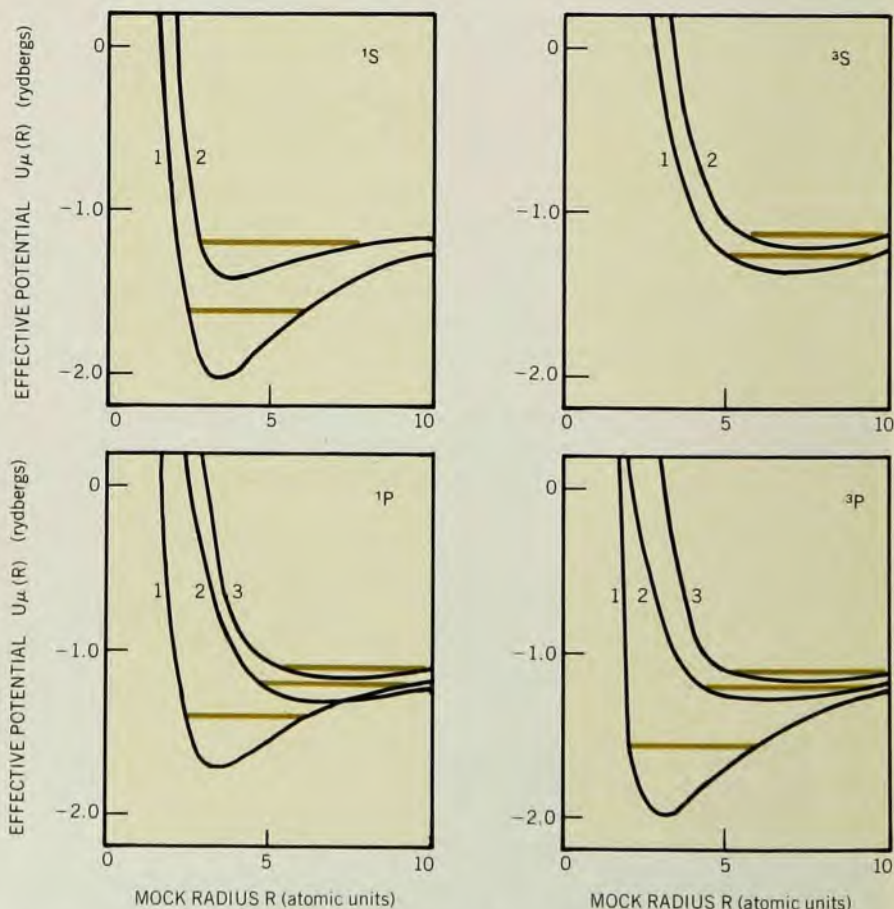
The presence of nodes in the dependence of the wave function on the coordinate R corresponds to excitation of joint (or "in-step") radial oscillations of the two electrons, such as were tentatively identified as characteristic of the most intense double excitations of helium. The presence of nodes in the dependence on α would instead correspond to the excitation of out-of-step radial oscillations of the two electrons, already tentatively as-

sociated with the fainter spectral series.

Using these coordinates and atomic units, one can write the Schrödinger equation for a two-electron atom, shorn of spin-orbit coupling, in the form:

$$\left\{ \frac{d^2}{dR^2} - \frac{1}{R^2} \right. \\ \times \left[-\frac{d^2}{d\alpha^2} - \frac{1}{4} + \frac{I_1^2}{\cos^2 \alpha} + \frac{I_2^2}{\sin^2 \alpha} \right] \\ \left. - \frac{1}{R} C(\alpha, \theta_{12}) + 2E \right\} \\ (R^{5/2} \sin \alpha \cos \alpha \Psi) = 0 \quad (3)$$

The structure of this equation is central for our analysis. (For a clearer exposition of the structure, refer to the Box, page 34—which also includes some analytic details of the work to be described below.) Its first term, d^2/dR^2 , corresponds to the kinetic energy associated with expansion or contraction of the atom as a whole. The second group of terms, inversely proportional to R^2 , consists of derivatives with respect to angular coordinates; here I_1^2 and I_2^2 are the orbital momentum operators of the two electrons and their contributions to the Hamiltonian correspond to the kinetic energy of angular motion, which reacts on variations of R as a centrifugal potential. The operator derivative with respect to the mock-angle



Macek's results for the "effective potential" $U_\mu(R)$ in equation 5 plotted against scale function R for $1S^0, 3S^0, 1P^0$ cases. The zeroth curve (the ground state) is not shown. The positions of the lowest member of the Rydberg series of autoionizing states for each curve is shown by the horizontal colored lines. (From J. H. Macek, *J. Phys. B*, **1**, 831, 1968.)

Figure 4

α may be regarded as a squared mock-angular momentum with effects analogous to those of orbital momentum. Finally, the total electrostatic interaction of nucleus and electrons is inversely proportional to R , for dimensional reasons. Its coefficient $C(\alpha, \theta_{12})$ depends on two variables only, which identify the relative position of the particles represented by the shape of the triangle in figure 3a. The factors in the parentheses with Ψ serve only to simplify the equation.

Note that this Hamiltonian for helium consists of three terms, proportional to d^2/dR^2 , $1/R^2$, and $1/R$, just as one finds in the radial Hamiltonian of the hydrogen atom. Here, however, the coefficients of $1/R^2$ and $1/R$ do not commute. This structure holds for any larger system consisting of nuclei and electrons. The expectation value of the coefficient of $1/R^2$ is positive, that of the coefficient of $1/R$ is generally negative (because $-C(\alpha, \theta_{12})$ is positive only in a narrow range of variables, as we will see later in figure 6). The first of these terms prevails at small R , the second at large R ; the resulting minimum of $\langle U(R) \rangle$ at intermediate R governs the size of the system.

Two initial clues were available to analyze equation 3:

- ▶ the coordinate R relates to the tentative characterization of the observed intense double excitation in helium, and
- ▶ the wavefunctions of successive excited states of the same series should have similar correlation patterns while extending to increasingly large distances R . These clues led Joseph Macek in 1966 to assume that the R coordinate might be approximately separable from the others and to construct approximate eigenfunctions of double excited states:

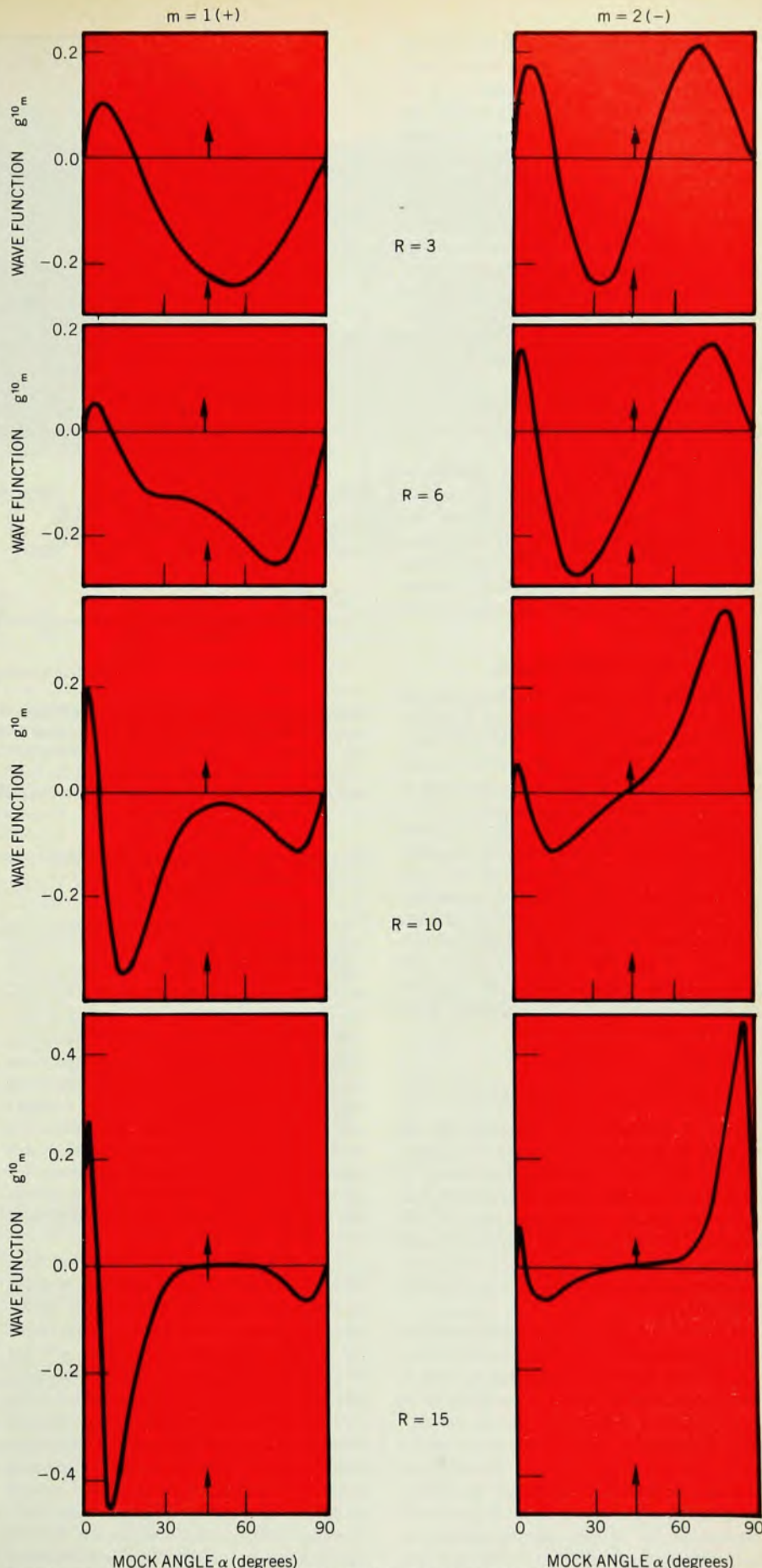
$$R^{5/2} \sin \alpha \cos \alpha \Psi_{\mu n} \approx \Phi_{\mu}(R; \alpha, \hat{\mathbf{r}}_1, \hat{\mathbf{r}}_2) F_{\mu_n}(R) \quad (4)$$

Here Φ_{μ} is an eigenfunction of the operator $U(R)$ of equation 3, that is, of the Schrödinger equation that results by freezing the coordinate R to a specified value, much as one freezes the internuclear distances in the study of molecular electrons. The index μ labels successive eigenvalues $U_{\mu}(R)$ of the restricted equation. The $F_{\mu_n}(R)$ are eigenfunctions of the approximate wave equation that remains after $U(R)$ is diagonalized in equation 3 and after the restriction to fixed R has been lifted, namely,

$$\left\{ \frac{d^2}{dR^2} - U_{\mu}(R) + 2E_{\mu_n} \right\} F_{\mu_n}(R) = 0 \quad (5)$$

Here $U_{\mu}(R)$ acts as an "effective potential." Equation 5 disregards the coupling of equations with different values of μ , as indicated in the box on page 34.

Macek obtained several of the lowest eigenvalues $U_{\mu}(R)$ numerically for a few sets of quantum numbers (S, L , parity) and then solved the corresponding equation 5, also numerically. Figure 4 shows



Solutions by C. D. Lin for the wave function $g^{10}(\alpha)$ of equation 6, for states in which the He^+ ion is excited to its $n = 2$ level (2s or 2p) at four different (fixed) values of R : 3, 6, 10 and 15 atomic units. (From *The Physics of Electronic and Atomic Collisions* (Invited papers from the IX ICPEAC, Seattle, Wash. 1975), Univ. of Washington Press, 1976; page 34.)

Figure 5

his results on which are overlaid some of the energy levels E_n^μ . Each sequence of eigenvalues E_n^μ with the same $(\mu, S, L, \text{parity})$ was found to coincide within acceptable error limits with one of the series of doubly excited He^{**} levels that had been previously observed or calculated by other methods. The goal was thus achieved of producing levels pre-grouped in Rydberg series, in contrast to earlier dependence on *ex-post-facto* analysis. Sample estimations showed the neglected coupling terms to be in fact small. These results also showed why the probabilities of excitation and autoionization of different series differ greatly, in general agreement with other evidence.

The success was limited, however, in that the calculation failed to provide the eigenfunctions Φ_μ in a form accessible to qualitative analysis, and hence it did not permit a physical interpretation of the quantum number μ that labels each series. Also the method had been developed from tenuous heuristic leads and its success could be estimated only by evaluation of its end products.

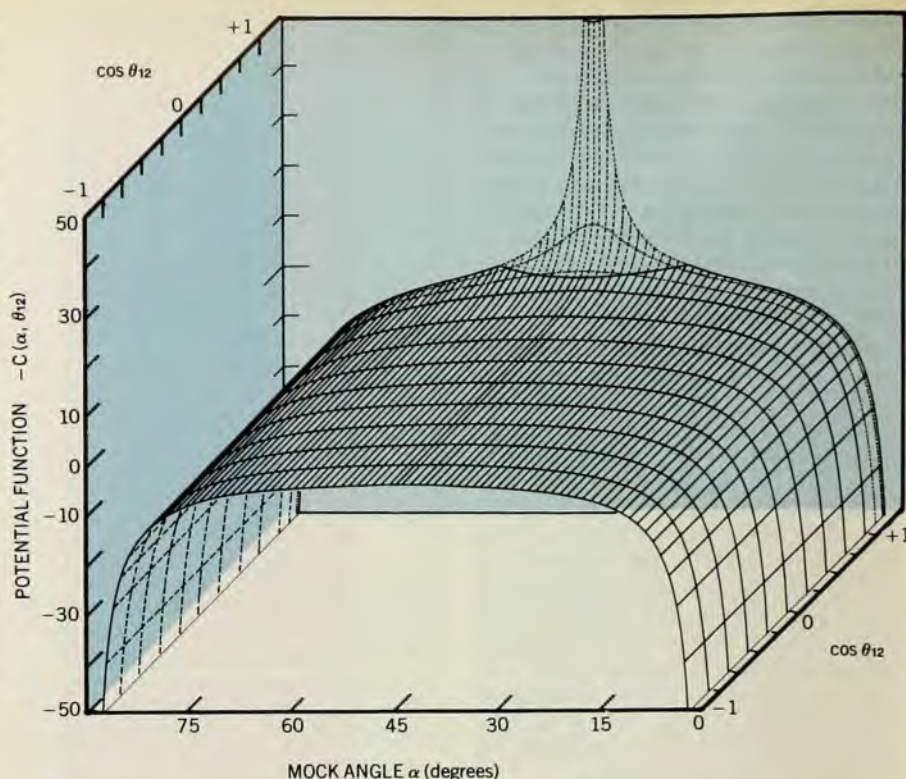
Full separation of coordinates

The search for an interpretation of Macek's results was resumed more recently by Chii-Dong Lin. He noticed at the outset that the repulsion between two electrons is less effective, in general, in altering their orbital momenta than in producing radial correlations. More specifically, matrix elements of the coefficient $C(\alpha, \theta_{12})$ of equation 4 that are off-diagonal in the orbital quantum numbers (l_1, l_2) are half an order of magnitude smaller than the diagonal elements. A zeroth approximation may then neglect initially these off-diagonal elements, casting Macek's angular wave functions in the form

$$\Phi_\mu \approx \Phi_{l_1 l_2 m}(R; \alpha, \hat{\mathbf{r}}_1, \hat{\mathbf{r}}_2) \\ = \mathcal{A} g^{l_1 l_2 m}(R; \alpha) Y_{l_1 l_2 L M}(\hat{\mathbf{r}}_1, \hat{\mathbf{r}}_2) \quad (6)$$

Here Y indicates a combination of spherical harmonics $Y_{l_1 m_1}(\hat{\mathbf{r}}_1) Y_{l_2 m_2}(\hat{\mathbf{r}}_2)$ with total orbital quantum numbers LM , \mathcal{A} is an antisymmetrization operator, and $g^{l_1 l_2 m}(R; \alpha)$ is an eigenfunction of the operator $U(R)$ of equation 3 averaged over $(\hat{\mathbf{r}}_1, \hat{\mathbf{r}}_2)$ with weight $(Y_{l_1 l_2 L M})^2$ and thus reduced to be a function of α and of the parameter R .

Equation 6 has the immediate effects of separating the variable α and of introducing the quantum number m , which indicates the number of nodes of the wave function $g^{l_1 l_2 m}$. The numerical calculation of this wave function, for given values of (l_1, l_2) and R , amounts to the solution of a single-variable Schrödinger equation, with eigenvalues $U_{l_1 l_2 m}(R)$. Equation 6 completes, in effect, the approximate separation of all six components of the two position vectors $(\mathbf{r}_1, \mathbf{r}_2)$ and, together with equation 4, classifies approximate stationary states by a maximal set of six quantum numbers (l_1, l_2, L, M, m, n) .



Relief map of the potential-energy coefficient $-C(\alpha, \theta_{12})$ for H^- ($Z=1$). Note the large negative values of the potential energy where α is near 0° and 90° , which is where either electron approaches the nucleus, and the flat saddle at $\theta_{12} = 180^\circ$, where the electrons lie on opposite sides of the nucleus. The sharp spike centered at $\theta_{12} = 0^\circ$, $\alpha = 45^\circ$, represents the condition where the two electrons approach each other. (From C. D. Lin, *Phys. Rev. A* **10**, 1990 (1974).) Figure 6

The angular correlation in these states is characterized by the coupling of (l_1, l_2) that yields the total orbital momentum L . The radial correlation is represented by the wave functions $g^{l_1 l_2 m}(R, \alpha)$ and $F^{l_1 l_2 m}_n(R)$. The angular and radial correlations are independent in this approximation but they are in fact interlinked insofar as a good approximation to Macek's wave functions Φ_μ requires the superposition of different wave functions (equation 6) with coefficients of comparable magnitude. This circumstance occurs only when different zeroth-order eigenvalues $U_{l_1 l_2 m}$ become degenerate for particular values of R ; the resulting effects are conspicuous but need not be discussed here.

The main results to be presented here emerge from a discussion of sample wavefunctions $g^{l_1 l_2 m}$ and of the corresponding eigenvalues $U_{l_1 l_2 m}$. We begin by considering wave functions g^{10} for large values of R and for excitation energies large but insufficient to detach both electrons from a helium atom. In this case the complete wave function must represent a He^+ ion in an s or p state and another electron in a p or s orbital loosely attached to or even detached from He^+ . Because the electron within the He^+ is much closer to the nucleus than the other electron, the wave function should be restricted in practice to values of α near 0° or 90° depending on whether electron number 2 or number 1 belongs to He^+ . It



can be seen from figure 3b that in our case the function g^{10} represents the radial wave function of the He^+ electron, whereas that of the other electron is represented by the factor $F^{10}_n(R)$ of equation 4, which does not concern us at the moment. Figure 5 shows plots of $g^{10}(\alpha)$ for states that consist, at large R , of a He^+ ion excited to its $n=2$ level (2s or 2p) and an electron further away from the nucleus. Indeed this function approaches a hydrogenic 2s function at low α and a 2p function at $\alpha \approx 90^\circ$. (The correspondence of 2s to low α , that is, to electron number 2, results here from an arbitrary convention and is removed by the antisymmetrization operator \mathcal{A} in equation 6.)

The essential point for us, shown in figure 5, is that two different functions, g^{10}_1 and g^{10}_2 , are obtained for the same limiting case of He^+ in its $n=2$ level. Both of them reduce to 2s and 2p in the alternative ranges of α , but they differ by the absence or presence of a node in the intermediate range of α and hence by their relative sign in the extreme ranges. We see here a formal analogy with the LCAO ("linear combination of atomic orbitals") molecular orbitals that are formed when two atoms begin to approach. In our case, the 2s and 2p levels of He^+ are degenerate and so are the eigenvalues U_{101} and U_{102} in the large- R limit; the energetic degeneracy would fail for a many-electron system but the qual-



The Brookdeal 9503 Family

A precision Lock-in Amplifier, offering "True Correlation" mode, "Fundamental Only" mode and a wide range of optional slot-ins.

Precision Lock-in	In both performance and price the 9503 stands comparison with any other lock-in on the market.	We've listed its most important specifications on the right.	<p>Basic specifications</p> <p>Sensitivity 1μV-500mV Frequency response: 2Hz-100kHz (0.2Hz-200kHz option) Maximum system overload: x 650,000 Maximum demodulator overload: 70dB (x 3000) (for 10V full scale) True differential 100M Ohms input <10nV/Hz input noise 6 position hi/lo pass filters 200 ppm/°C gain stability 10 ppm/°C zero stability 0.03° rms phase stability 0.005° rms phase jitter 10 volt output ~20μs-100s time constant (option to give 12dB/octave roll-off) 10 turn vernier phase adjustment 10 turn vernier zero offset Display bus Phase lock mode Hi stability mode Hi dynamic reserve mode Transient noise suppression option 2f mode Function check</p>
Three operating modes	You can use the 9503SC as a straight lock-in amplifier, or in "true correlation" mode, or in "fundamental only" mode (more about these below.) You can also buy the 9503C	as a straightforward precision lock-in, with true correlation mode. And of course, there is the 9503 straight lock-in—the other modes can be added later if you need them.	
Ten Slot-ins	The growing family of Brookdeal slot-ins gives you the best measurement for any application, in the most cost-effective way. At present there are 6 pre-amps, 1 filter, an omniphase unit, an internal oscillator and a ratiometer. Each one is reasonably priced and individually available as required. Ask for full details.	 	
True Correlation	True correlation is a feature exclusive to Brookdeal. It provides superior signal-to-noise ratios, particularly from pulsed or irregularly shaped signals. It also allows you to make very fast swept frequency measurements.	Based on carrier pulse modulation techniques, the system responds to the frequency distribution of signal energy, behaving as a matched detector.	
Fundamental only	This function gives harmonic suppression over a wide frequency range, and is based on a special carrier pulse modulation technique which Brookdeal call "Sinetrac."	It's particularly useful for precision ac bridge measurements and low frequency measurements where there are discrete interference frequencies.	

Brookdeal Electronics Ltd
Doncastle House
Doncastle Road Bracknell
Berks. RG12 4PG
England
Tel (0344) 23931 Telex 847164

Ortec Inc	100 Midland Road Oak Ridge Tennessee 37830 Tel (615) 482-4411 Telex 055-7450	France Ortec SARL Paris Tel 283 1256 Telex 685083	Italy Ortec SpA Milan Tel 738 6294 Telex 34377	Germany Ortec GmbH Munich Tel (089) 98 71 73 Telex 528257
-----------	--	---	--	---

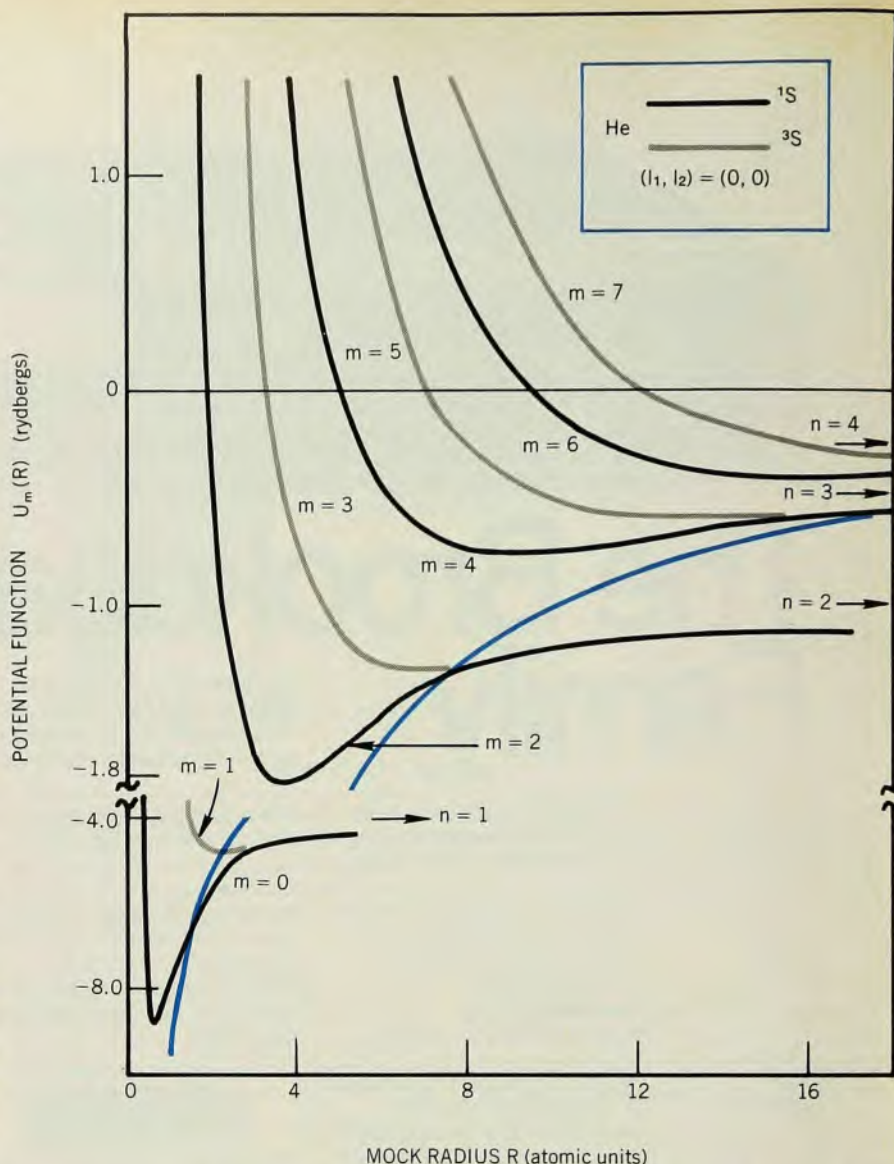
**ORTEC
Brookdeal**

0000

itative pattern of the wave functions $g^{l_1 l_2}_m(\alpha)$ at large R should normally be preserved, as it is in the molecular analogue.

The plots of figure 5 for the largest value of R , namely, 15 atomic units, resemble those of the wave function for a single particle in a pair of potential wells separated by a barrier. Those for lower values of R resemble increasingly the orbitals of a particle in a single potential well. This behavior is readily interpreted from a consideration of the structure of equation 3 and of its potential-energy coefficient $C(\alpha, \theta_{12})$ which is mapped in figure 6. The map shows large negative values of the potential energy concentrated in two ditches, at α near 0° or 90° , which correspond to close approach of either electron to the nucleus. These ditches are separated by a broad barrier at $\alpha \approx 45^\circ$, which is topped by a flat saddle at $\theta_{12} = 180^\circ$, where the electrons lie on opposite sides of the nucleus, and by a sharp spike at $\theta_{12} \approx 0^\circ$, where the two electrons approach each other. The spike is smoothed out by the averaging over θ_{12} which precedes the calculation of $g^{l_1 l_2}_m$; this function is thus governed by an effective potential consisting of two wells separated by a barrier. The dependence of $g^{l_1 l_2}_m$ on R results then from the relative magnitude of the coefficients, $1/R^2$ and $1/R$, of the kinetic and potential terms of the operator $U(R)$. At large R the attractive potential energy predominates; it causes the eigenvalue $U_{l_1 l_2 m}$ to be negative and it confines the wavefunction within the two wells on either side of the barrier. At small R the positive kinetic energy predominates and causes the eigenvalue to be positive, thus rising above the barrier, and the wavefunction to oscillate throughout the range of α .

Figure 7 shows a sample plot of eigenvalues $U_{l_1 l_2 m}(R)$, which are positive for small R and negative for large R , as expected. A minimum of $U(R)$ generally occurs for helium at a value for R a little smaller than the value at which U becomes lower than the potential's saddle, $-C(45^\circ, 180^\circ)/R$. The large- R limit of U coincides with an energy level of the He^+ ion. As noted above, each eigenvalue $U(R)$ acts as a potential function in the radial Schrödinger equation (equation 5). In particular, the deepest potential well in figure 7 represents the forces that bind



Potential energy curves for s^2 states of helium. Note the intersections with the colored line, which represents the level of the potential saddle in the map of figure 6—that is, the value of $-C$ at $\alpha = 45^\circ$, $\theta_{12} = 180^\circ$. The large- R limit of U coincides with an energy level of the He^+ ion. (From C. D. Lin, *loc. cit.*, page 1995.)

Figure 7

the electron pair of the helium atom in its ground state. After corrections for the inaccuracy of Lin's approximate equation 6, this approach yields surprisingly accurate binding energies for He and for H^- .

Potential saddle

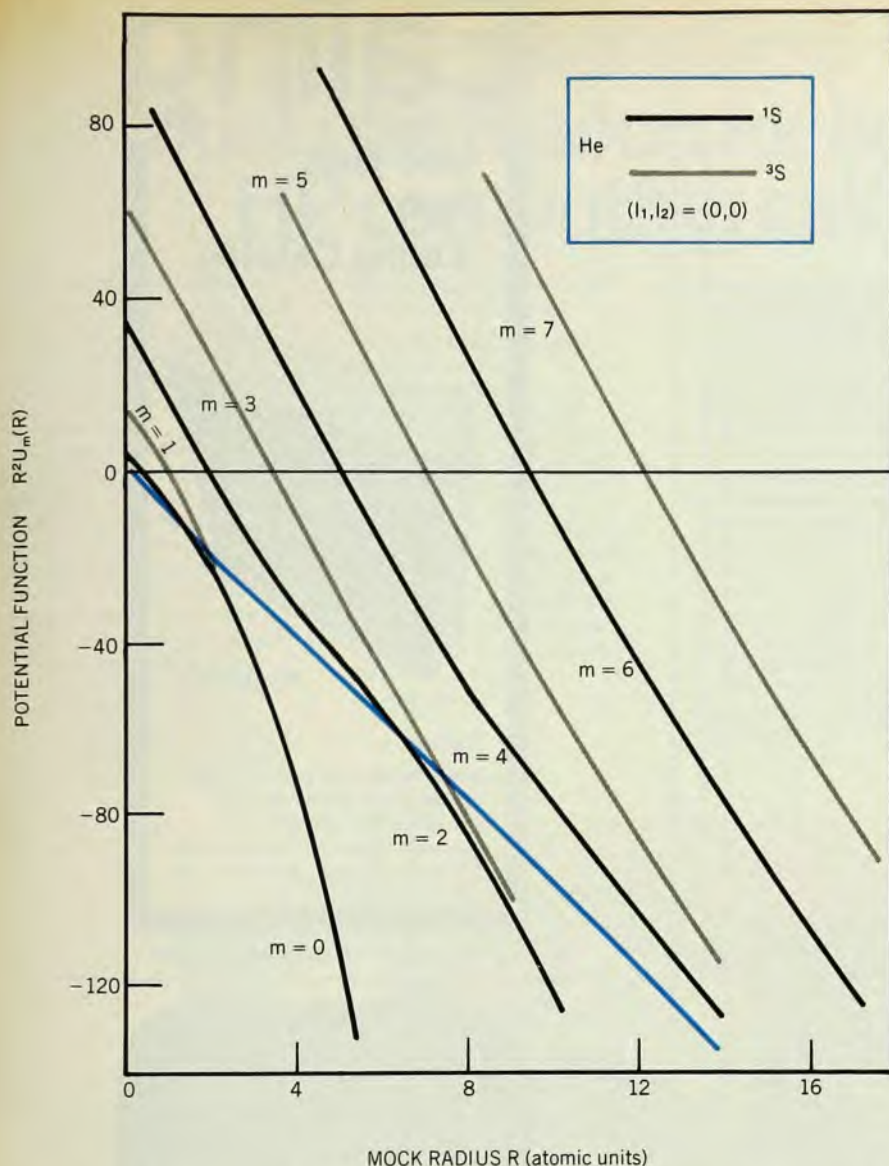
Each of the separable approximate wavefunctions represents, at large R , a He^+ ion in a certain energy level and a distant electron. Accordingly the description of an excitation process must involve a superposition of different separable wave functions, represented at large R by one ingoing term $\Phi_\mu(R; \alpha, \hat{\mathbf{r}}_1, \hat{\mathbf{r}}_2) \exp(-ik_\mu R)$ and by outgoing waves $\Sigma_\mu A_\mu \Phi_\mu(R; \alpha, \hat{\mathbf{r}}_1, \hat{\mathbf{r}}_2) \exp(ik_\mu R)$, where the existence of nonzero coefficients A_μ with $\mu' \neq \mu$ results from the coupling terms shown in the box on page 34. That these coupling terms are generally small ap-

pears to stem from the smooth dependence on R of the different terms of equation 3. Analogy with molecular processes suggests that the coupling terms may be most important for particular values of R at which different eigenvalues $U_\mu(R)$ are more nearly degenerate, approaching each other in a pattern of "avoided crossing." This circumstance would localize the electronic excitation process in such ranges of R . Figure 7 shows that each curve tends to approach the next one of the same set near its intersection with the level of the potential saddle, as it begins to rise while the next curve is still descending toward its minimum. This systematic trend is displayed more strikingly by plotting the product $R^2 U_{l_1 l_2 m}$ instead of $U_{l_1 l_2 m}$ itself (figure 8). The product has a finite positive value at $R = 0$ and then decreases at small R as $\langle -C(\alpha, \theta_{12}) \rangle_{l_1 l_2 m} R$. At large R , where U

For further reading . . .

More extensive reviews of the material presented in this article, including references to the original literature, are found in the author's publications:

- *Atomic Physics* 1, 209 (1969) and 4, 47 (1975); Plenum, N.Y.
- "Photoionization and Other Probes of Many-Electron Interactions," in press (Plenum, N.Y.).



The systematic trend shown by the intersections of the curves of figure 6 with the colored line of that figure is made more striking in this replot of the same data with ordinate $R^2 U_{l_1 l_2 m}$. The transition from a linear to a parabolic trend in the lines of $R^2 U$ occurs near the intersection with the potential-saddle line (again shown in color). (From C. D. Lin, *loc. cit.* page 1995.)

Figure 8

approaches an energy level of He^+ , the product takes the parabolic trend $E(\text{He}^+)R^2$. The transition from a linear to a parabolic trend occurs near the intersection with the potential saddle line; it is rather abrupt and marked by avoided crossings for the $1S$ family of curves while it is much smoother for the $3S$ curves.

These results are readily interpreted in terms of the structure of the coupling terms $W_{\mu\mu'}$ shown in the box on page 34. Each eigenfunction $g^{l_1 l_2 m}(R; \alpha)$, as well as the more accurate $\Phi_\mu(R; \alpha, \hat{\mathbf{r}}_1, \hat{\mathbf{r}}_2)$, may vary smoothly over most of the range of R , with small derivative $\partial\Phi_\mu/\partial R$; however it must drop rapidly to small values in the saddle point region ($\alpha \approx 45^\circ$) as R increases through the range where the eigenvalue U drops below the level of the potential saddle. Sample evaluation of coefficients $W_{\mu\mu'}$ confirms that their values peak in this range of R . The dif-

ferent behavior of $1S$ and $3S$ curves is accounted for by noting that the $3S$ wave functions must vanish for symmetry reasons at $\alpha = 45^\circ$ and thus are never large in the saddle region, whereas the $1S$ functions have an antinode there for small R . We find here a selection rule stating that transition probabilities are smaller for $3S$ than for $1S$ states.

The peaking of coupling coefficients as the eigenvalues traverse the level of the potential saddle, and the strong dependence of their peak values on the presence of an antinode rather than a node near the saddle position ($\alpha = 45^\circ$), appear to have general significance. The occurrence of an antinode or node is correlated with singlet or triplet character for S states only. For $1P^0$ states, for example, one finds an antinode or a node for alternate states with the same (S, L , parity). Figure 5, for example, shows how the two

wave functions g^{10}_1 and g^{10}_2 differ in this respect. In a plot analogous to figure 8 for the set of $1P^0$ eigenvalues, the curves with $m = 1, 3, 5 \dots$ show rather sharp avoided crossings as the $1S$ curves do in figure 8, while those with $m = 2, 4, 6 \dots$ are smoother like the $3S$ curves. These results confirm and extend the early tentative interpretation of the occurrence of strong and faint Rydberg series of resonances in the photoabsorption spectrum of helium.

Present state: future plans

The qualitative results we have described rest on *dimensional* and *topological* considerations that apply to systems consisting of any number of nuclei and electrons. The Schrödinger equation (3) is expressed in terms of a single dimensional coordinate R ranging from zero to infinity and of angular and mock-angular coordinates with a finite range. On these grounds alone, the operator U has a *discrete spectrum* and consists of a kinetic energy term proportional to $1/R^2$ and of a potential energy term proportional to $1/R$. The multivariable potential-energy function C reaches minus infinity and plus infinity at different sets of points and must, therefore, have saddle points. When one particle is far away from the others, the wave function should be concentrated in potential wells separated by barriers, while remaining connected across each barrier by a tail that may or may not include a node, as it does in figure 5; the eigenvalues of U for states with and without such a node are nearly degenerate. Accordingly, the dynamical effects resulting from these circumstances should be similar for different aggregates.

Numerical applications of the computational approach outlined in this paper have not yet been very extensive and have been semi-quantitative rather than accurate. Higher priority is being given to a search for a basis set of wave functions Φ_μ that minimizes the pair of coupling terms $U_{\mu\mu'}$ and $W_{\mu\mu'}$ shown in the box on page 34, as compared to the $W_{\mu\mu'}$ constructed with the eigenvectors of the operator U . Another important question to be explored is the connection between the approximate factorization $\Phi_\mu(R; \Omega)F_n(R)$ considered here for the study of comparatively low levels of double excitation and an alternative factorization that has been introduced in a study of double detachment by G. H. Wannier, A. R. P. Rau and R. K. Peterkop; this process also hinges on the behavior of wavefunctions in the saddle-point region of the potential.

* * *

This article is an adaptation, by the author, of the text of his talk given at the April 1976 meeting of The American Physical Society, in Washington D.C., when he was presented with the Davison-Germer Prize. □